TRIUMF — RESEARCH PROPOSAL	Experiment no.	Sheet 1 of 32

Title of proposed experiment:

Weak nucleon-nucleon interactions by parity non-conservation measurements in francium

Name of group: FrPNC

Spokesperson for group: Gerald Gwinner

E-Mail address: gwinner@physics.umanitoba.ca Fax number: (204) 474-7622

Members of the group (name, institution, status, per cent of time devoted to experiment)

Name	Institution	Status	Time
G.D. Sprouse	Stony Brook University	Professor	30%
J.A. Behr	TRIUMF	Research Scientist	40%
K.P. Jackson	TRIUMF	Research Scientist	10%
M.R. Pearson	TRIUMF	Research Scientist	40%
TRINAT student	University of British Columbia	Grad Student	100%
G. Gwinner	University of Manitoba	Professor	40%
Student	University of Manitoba	Grad Student	100%
L.A. Orozco	University of Maryland	Professor	30%
Student	University of Maryland	Grad Student	100%
Postdoctoral Associate	University of Maryland	Postdoctoral Associate	100%
V. Flambaum	University of New South Wales	Professor (theory)	20%
S. Aubin	University of Toronto	Postdoctoral Associate	10%

Start of preparations: 2006

Date ready: when Fr beams are available

Completion date: 5 years after starting

Beam time requested:

12-hr shifts	Beam line/channel	Polarized primary beam?
200	BL2A/ISAC	No

The researchers will conduct a measurement of the anapole moment in Fr. The anapole moment of a nucleus is a parity non-conserving (PNC), time reversal conserving moment that arises from weak interactions between the nucleons. Its measurement is a unique probe for neutral weak interactions inside the nucleus. The anapole can be detected in a PNC electron-nucleus interaction and reveals itself as a nuclear-spin dependent signal. The proposed measurement of the nuclear anapole moment will be by direct excitation of an E1 transition within the ground state hyperfine manifold. This transition is parity forbidden, but is allowed by the anapole-induced mixing of opposite parity states.

This proposal combines precision measurement techniques from atomic, molecular and optical physics with the forefront understanding of low-energy nuclear structure for the elucidation of the weak interaction in a chain of Fr isotopes, where the effect is predicted to be one order of magnitude larger than in Cs. We will place $\approx 10^6$ trapped atoms at the anti-node of a standing microwave/RF field and measure the population transferred by the parity forbidden E1 transition. A highly synergetic, optical parity experiment will complement the microwave/RF measurement.

The project will have as a first benchmark the laser trapping and cooling of Fr atoms on-line at ISAC. The researchers have ample experience in the construction, commissioning and operation of magneto-optical traps for francium. The second step will require the transport and confinement of the trapped atoms into a region of controlled electric and magnetic fields to interrogate the atoms. The TRINAT collaboration has experience in such transfer of radioactive atoms. This environment will allow us to detect the PNC signature. Extensive studies of systematic effects will ultimately permit the extraction of the anapole moments of Fr isotopes with 10 % accuracy, constraining parity non-conserving meson-nucleon couplings. In particular, measurements in isotopes with unpaired neutrons will be sensitive to a different combination of weak meson-nucleon couplings compared to the one extracted from Cs and Tl data.

Experimental area

An electromagnetically shielded, temperature-controlled room in a location to be determined in the ISAC low-energy area.

Primary beam and target (energy, energy spread, intensity, pulse characteristics, emittance)

500 MeV protons, unpolarized;
UC_2 or ThC_2 target, 1–100 μA protons;

Secondary channel ISAC LEBT

Secondary beam (particle type, momentum range, momentum bite, solid angle, spot size, emmittance, intensity, beam purity, target, special characteristics)

Mass-separated $\leq$ 30 keV, isotopically clean francium ion beams from ISAC;

TRIUMF SUPPORT:

- Beam line to deliver ≤ 10 keV francium ions to a neutralizer.
- Electromagnetically shielded enclosure in experimental hall with temperature control and air filter for lasers and rf equipment, 5.5 m by 6 m.
- Mechanical design help for radiation shielding in the neutralizer region.

NON-TRIUMF SUPPORT

- NSERC, *Tests of fundamental symmetries with ultra-cold radioactive atoms and cold ions in traps and storage rings* (G. Gwinner); support has been granted through April 2006; continuing support through April 2008 has been applied for.
- NSF (USA) *Anapole moment studies in francium* (L. A. Orozco); support has been granted through June 2007.
- NSERC TRINAT project grant (J.A. Behr, K.P. Jackson, M. Pearson); support has been granted through April 2006; continuing support through 2009 has been applied for.

Yields of $> 10^8$ /sec short-lived Fr alpha emitters will be delivered to the main ISAC floor. Most of the activity is alpha radiation and will be contained in the trap region. Mechnical design support will be requested for lead or heavymet shielding near the trap volume. Mechanical pump exhausts will be filtered using the experience gained from the E929 radon EDM experiment tests with xenon. Certain masses produce long-lived ^{206,208,209,210}Po and will require careful precautions as polonium is quite volatile. The safety officer will be M. Pearson, who has experience gained at experiments at ISOLDE and at Stony Brook.

1 Scientific Justification

Parity non-conservation (PNC) in atoms comes from two types of interaction: Nuclear spin independent and nuclear spin dependent [1]. Nuclear spin dependent PNC occurs in three ways [2,3]: An electron interacts weakly with individual valence nucleons (nucleon axial-vector current $A_n V_e$), the nuclear chiral current created by weak interactions between nucleons (anapole moment), and the combined action of the hyperfine interaction and the spin-independent Z^0 exchange interaction from nuclear vector currents $(V_n A_e)$. [4–6].

Zel'dovich first proposed the existence of the nuclear anapole moment in 1957 [7]. Vetter *et al.* [8] obtained a limit for its value in thallium, and it was measured with an accuracy of 15% through the hyperfine dependence of atomic parity non-conservation in cesium by Wood *et al.* [9,10]. In this proposal, we present the feasibility of measuring the anapole moment through the electric dipole transitions it induces within the ground state hyperfine manifold in alkali atoms held in a dipole trap. Since the anapole moment scales as $Z^{2/3}$ and the matrix element scales as Z^2, with Z the atomic number, we focus our study primarily on francium isotopes, the heaviest of the alkali atoms [11]. Recent work related to time-reversal invariance and parity violation tests in traps [12–14] points to the many potential advantages of combining traps with tests of fundamental symmetries, but also highlights the systematics errors present in such measurements.

We propose a measurement of the nuclear anapole moment by direct excitation of the microwave E1 transition between and or within the ground hyperfine states of an alkali atom. The transition is parity forbidden, but is allowed by the anapole induced mixing of opposite parity states. The general approach has been suggested and followed for atomic PNC measurements in the past [15–21]. We modify the idea of Fortson [22] for atomic PNC with an ion placed at the anti-node of a standing optical wave by placing many trapped atoms at the anti-node of a standing microwave field. The stability requirements for the field and the interrogated sample are relaxed given the microwave wavelength. The measurement of an anapole moment in Cs shows that atomic PNC is a significant probe for neutral weak interactions inside the nucleus [4,23,24].

An optical PNC experiment based on the highly successful work by Wieman and coworkers [9] naturally fits the scientific goals this proposal. Our collaboration is giving serious thought to such a measurement to include it into the design of the apparatus from the beginning. A PNC-induced E1 transition from $7s$ to $8s$ in a trapped sample of Fr placed in a high-finesse optical cavity will provide an additional route to measure the anapole with different systematic effects.

This proposal is the beginning of a series of proposals that the collaboration will submit. They all relate to physics with Fr. We expect to submit separately a proposal to measure the M1 strength in the francium $7s \rightarrow 8s$ transition, and also for an optical atomic parity experiment to test weak neutral quark-lepton couplings, with full physics justification and plan for such an experiment in that proposal.

1.1 Parity non-conservation

Parity non-conservation was measured for the first time in three experiments with weak charged currents in 1957 [25–27]. Attempts to unify the weak and electromagnetic interactions by Weinberg [28], Salam [29], and Glashow [30] showed the existence of a neutral heavy boson associated with the weak interaction. The effects of a neutral boson in atomic PNC had already been esti-

mated years before by Zel'dovich [2]. The race for the detection of the consequences for neutral currents started and the high energy community with the Gargamelle experiment at CERN saw a positive signature in the elastic muon-neutrino electron scattering [31]. The neutral weak interaction between the electron and the nucleons remained to be observed since it is dominated by the electromagnetic interaction. It was first observed in atomic PNC experiments [32–35] in 1978. Further experiments in high energy physics with inelastic scattering enhanced the evidence of the neutral electroweak interaction [36]. The particles responsible for the weak interaction (W^+, W^-, and Z^0) were observed in 1983 [37,38].

Atomic PNC experiments, such as the Boulder one performed in cesium [10], measure an electric dipole transition rate between levels of the same parity. The extraction of weak interaction parameters from a PNC measurement requires the calculation of a matrix element that contains a weak interaction operator, energy levels coming from perturbation theory, and polarizabilities (sums of electric dipole transition matrix elements). These quantities are sensitive to the electron wave functions at short, intermediate and large distances from the nucleus, respectively. The energy levels and electric dipole transition matrix elements can be determined directly from spectroscopy. Unfortunately, the weak interaction matrix element cannot be measured directly. Instead, the Boulder cesium PNC experiment measures the product of the weak matrix element with the weak charge. Since the interest is in extracting the weak charge, it is necessary to rely on a theoretical calculation of the weak matrix element. The short range weak interaction depends on the electron density at the nucleus.

The improvement in precision of the PNC measurement in cesium [9,10] encouraged theorists to revisit their calculations to account for previously neglected corrections. The availability of high precision spectroscopic measurements made it possible to compare their predictions with measurements to below 1%. Several new corrections had to be included such as the Breit interaction [39], the strong-field radiative corrections [40,41], and the self-energy and vertex contribution [42,43]. The relevance of the corrections will be different depending on the atom which is why atomic physics measurements in francium are not only important for a future PNC measurement in francium, but also as a cross check for calculations in cesium.

The interaction between an electron and a nucleon can be mediated by a photon if it is electromagnetic, or by a Z^0 boson if it is weak according to the minimal standard model. Both the photon and Z^0 channels are comparable at high energy, while the Z^0 channel is suppressed at low energies by $q^2/M_{Z^0}^2$ with q the momentum transfer and M_{Z^0} the Z^0 boson mass [44]. The suppression appears because at low energies the interaction happens through virtual Z^0 bosons since there is not enough energy to create them. The experiments at low and high energies are sensitive to different quantities and become complementary. For example, electron scattering at the Z^0 pole can be used to obtain a value for the Weinberg angle, but if that value does not agree with the one extracted from atomic PNC measurements (after taking into account the running of $\sin^2\theta_W$), that could be an indication of physics beyond the standard model.

Peskin and Takeuchi introduced a parametrization of physics beyond the standard model in terms of two parameters, S and T [45,46]. Atomic PNC measurements are sensitive almost only to the S parameter and can be used in combination with other experiments to separate the S and the T contributions [6]. PNC measurements are particularly sensitive to extra Z bosons [44]. A crude estimate for the effect of an extra Z boson can be obtained from the suppression at low energies. In the case where the extra boson is identical to its lighter counterpart, the correction at low energies would be proportional to $M_{Z^0}^2/M_{Z_\chi}^2$ with M_{Z_χ} the mass of the extra boson. Since the precision of PNC measurements is $\sim$1% the crude estimate sets a lower bound of $M_{Z_\chi} >$

$10M_Z$ = 912 GeV. A careful analysis gives a lower bound for extra Z bosons from the cesium PNC measurement of $M_{Z_\chi} > 750$ GeV [6] which is higher than the 600 GeV limit set by direct searches at the Tevatron [47] and a global analysis including the experiments at LEP [48].

1.2 Atomic PNC theoretical background

The exchange of weak neutral currents between electrons and nucleons constitutes the main source of parity violating atomic transitions. There are two kinds, depending on whether the electron or nucleon current is of the axial type. The Hamiltonian for an infinitely heavy nucleon without radiative corrections is [49]

$$H = \frac{G}{\sqrt{2}} \left(\kappa_{1i} \gamma_5 - \kappa_{\text{nsd},i} \, \boldsymbol{\sigma}_n \cdot \boldsymbol{\alpha} \, \delta(\boldsymbol{r}) \right), \tag{1}$$

where $G = 10^{-5}$ m$_p^{-2}$ is the Fermi constant, m$_p$ is the proton mass, γ_5 and $\boldsymbol{\alpha}$ are Dirac matrices, $\boldsymbol{\sigma}_n$ are Pauli matrices, and κ_{1i} and $\kappa_{\text{nsd},i}$ are constants of the interaction with $i = p, n$ for a proton or a neutron, and 'nsd' stands for 'nuclear spin dependent'. The standard model tree level values (no loops included in the calculation) for these constants with $\kappa_{\text{nsd},i} = \kappa_{2i}$ are

$$\begin{aligned} \kappa_{1p} &= \frac{1}{2}(1 - 4\sin^2\theta_W), \ \kappa_{1n} = -\frac{1}{2}, \\ \kappa_{2p} &= -\kappa_{2n} = \kappa_2 = -\frac{1}{2}(1 - 4\sin^2\theta_W)\eta, \end{aligned} \tag{2}$$

with $\sin^2\theta_W \sim 0.23$ the Weinberg angle and $\eta = 1.25$. κ_{1i} (κ_{2i}) represents the coupling between nucleon and electron currents when the electron (nucleon) is the axial vector.

In an atom, the contribution from equation 1 for all the nucleons must be added. It is convenient to work in the shell model approximation with a single valence nucleon of unpaired spin. For the nuclear spin independent part ('nsi') we have

$$H_{\text{PNC}}^{\text{nsi}} = \frac{G}{\sqrt{2}} \frac{Q_W}{2} \, \gamma_5 \, \delta(\boldsymbol{r}), \tag{3}$$

which is proportional to the weak charge

$$Q_W = 2(\kappa_{1p} Z + \kappa_{1n} N), \tag{4}$$

with N the number of neutrons. Because of strong cancellation in κ_{1p}, the standard model value for the weak charge is almost equal to -N. The theoretical uncertainty present in all the extractions of weak interaction parameters from atomic PNC comes from the calculation of the matrix element γ_5 as the experiment is not sensitive to the weak charge itself but to the product as indicated in equation 3.

Looking at this last Hamiltonian, it is possible to follow more exactly the Z dependence of the interaction for an s state atom for which PNC mixes some p character into its ground s state. The s level wave function grows as $Z^{1/2}$ at the origin, the derivative (the momentum) of the p level at the origin scales as $Z^{3/2}$ and $Q_W \approx -N \approx -Z$ gives an overall scaling for the weak matrix element of $Z^3 R$, with R a relativistic enhancement factor. In a simple picture, the latter stems

from the increase of the relativistic momentum of the electron, as it approaches a heavy nucleus at relativistic speeds (see the book of Khriplovich for an extended explanation [49]). As an example, the PNC effect of the spin independent part should be 18 times larger in francium than in cesium according to the calculations of Refs. [50,51].

The second term of equation 1 is nuclear spin dependent ('nsd'), and due to the pairing of nucleons, its contribution has a weaker dependence on Z. The result after summing over all nucleons is [52]

$$H_{\rm PNC}^{\rm nsd} = \frac{G}{\sqrt{2}} \frac{K \boldsymbol{I} \cdot \boldsymbol{\alpha}}{I(I+1)} \kappa_{{\rm nsd},i} \delta(\mathbf{r}), \tag{5}$$

where $K = (I + 1/2)(-1)^{I+1/2-l}$, l is the valence nucleon orbital angular momentum, and I is the nuclear spin. The terms proportional to the anomalous magnetic moment of the nucleons and the electrons have been neglected.

The interaction constant is given by

$$\kappa_{{\rm nsd},i} = \kappa_{a,i} - \frac{K - 1/2}{K} \kappa_{2,i} + \frac{I+1}{K} \kappa_{Q_W}, \tag{6}$$

with $\kappa_{2,i}$ given by equation 2 corresponding to the tree level approximation, and we have two corrections, the effective constant of the anapole moment $\kappa_{a,i}$ and κ_{Q_W} that is generated by the nuclear spin independent part of the electron nucleon interaction together with the hyperfine interaction. Flambaum and Murray [52] showed that

$$\begin{aligned} \kappa_{a,i} &= \frac{9}{10} g_i \frac{\alpha \mu_i}{m_p \tilde{r_0}} \mathcal{A}^{2/3}, \\ \kappa_{Q_W} &= -\frac{1}{3} Q_W \frac{\alpha \mu_N}{m_p \tilde{r_0} \mathcal{A}} \mathcal{A}^{2/3}, \end{aligned} \tag{7}$$

where α is the fine structure constant, μ_i and μ_N are the magnetic moment of the valence nucleon and of the nucleus, respectively, in nuclear magnetons; $\tilde{r_0} = 1.2$ fm is the nucleon radius, $\mathcal{A} = Z + N$, and g_i gives the strength of the weak nucleon-nucleus potential with $g_p \sim 4$ for a proton and $0.2 < g_n < 1$ for a neutron [49]. The interaction is stronger in heavier atoms, since both $\kappa_{a,i}$ and κ_{Q_W} scale as $\mathcal{A}^{2/3}$ ($Q_W/\mathcal{A} \sim 1/2$ in κ_{Q_W}). The anapole moment is the dominant contribution to the interaction in heavy atoms, for example in ^{209}Fr, $\kappa_{a,p}/\kappa_{Q_W} \simeq 15$, so it is safe to assume that $\kappa_{{\rm nsd},i} = \kappa_{a,i}$. Arguments similar to the nuclear spin independent part give a scaling for the matrix element of the nuclear spin dependent part of $Z^{8/3}R$. The effect in francium in this case is 11 times larger than in cesium.

1.3 The anapole moment

The anapole moment of a nucleus is a parity non-conserving (PNC), time reversal conserving moment that arises from weak interactions between the nucleons (see the recent review by Haxton and Wieman [4]). It can be detected in a PNC electron-nucleus interaction and reveals itself in the spin-dependent part of the PNC interaction. Wood *et al.* [9,10] measured the anapole moment of ^{133}Cs by extracting the dependence of atomic PNC on the hyperfine energy levels involved, and consequently nuclear spin. The anapole moment is defined by (see [7])

$$\mathbf{a} = -\pi \int d^3 r r^2 \mathbf{J(r)}, \tag{8}$$

with **J** the electromagnetic current density. The anapole moment in francium arises mainly from the weak interaction between the valence nucleons and the core. It is possible to think of it as a weak radiative correction that is detectable only with an electromagnetic interaction. Flambaum, Khriplovich and Sushkov [3], by including weak interactions between nucleons in their calculation of the nuclear current density, estimate the anapole moment from equation 8 for a single valence nucleon to be

$$\mathbf{a} = \frac{1}{e}\frac{G}{\sqrt{2}}\frac{K\boldsymbol{j}}{j(j+1)}\kappa_{a,i} = C_i^{an}\boldsymbol{j}, \tag{9}$$

where j is the nucleon angular momentum. These values correspond to the nuclear values for the case of a single valence nucleon. The calculation is based on the shell model for the nucleus, under the assumption of homogeneous nuclear density and a core with zero angular momentum leaving the valence nucleon carrying all the angular momentum.

1.4 Status of atomic PNC measurements

The weak interaction in atoms induces a mixing of states of different parity, observable through PNC measurements. Transitions that were forbidden due to selection rules become allowed through the presence of the weak interaction. The transition amplitudes are generally small and an interference method is commonly used to measure them. A typical observable has the form

$$|A_{PC} + A_{PNC}|^2 = |A_{PC}|^2 + 2Re(A_{PC}A_{PNC}^*) + |A_{PNC}|^2, \tag{10}$$

where A_{PC} and A_{PNC} represent the parity conserving and parity non-conserving amplitudes. The second term on the right side corresponds to the interference term and can be isolated because it changes sign under a parity transformation. The last term is usually negligible.

All recent and on-going experiments in atomic PNC rely on the large heavy nucleus (large Z) enhancement factor proposed by the Bouchiats [53–55]. These experiments follow two main strategies (see recent review by M.-A. Bouchiat [56]). The first one is optical activity in an atomic vapor. The asymmetry introduced by PNC makes the atoms interact preferentially with right (or left) circularly polarized light. A linearly polarized light beam propagating through an atomic vapor experiences a rotation of the polarization plane analogous to the one observed in the Faraday effect except that in this case there is no magnetic field present. The measurement strategy uses interference with an allowed transition to enhance the small effect. The amount of rotation is related to the weak charge, which quantifies the effect of the weak force. The method has been applied to reach a precision of 2% in bismuth [57], 1.2% in lead [58,59] and 1.2% in thallium [8].

The second strategy measures the excitation rate of a highly forbidden transition. The electric dipole transition between the $6s$ and $7s$ levels in cesium becomes allowed through the weak interaction. Interference between this transition and the one induced by the Stark effect due to the presence of an static electric field generates a signal proportional to the weak charge. The best atomic PNC measurement to date uses this method to reach a precision of 0.35% [9,10]. The exquisite precision reached with the cesium experiment at Boulder allowed the extraction of the anapole moment from their measurement [9,10]. The transition is dominated by the spin independent contribution, which is proportional to the weak charge. They observed a small difference in the signal depending on the hyperfine levels used for the transition. The difference corresponds

to the spin dependent contribution which for cesium is dominated by the anapole moment. They extracted the spin dependent contribution with an accuracy of 14% giving the first unambiguous measurement of an anapole moment.

Other methods have been proposed and some work is already on the way. The Bouchiat group in Paris has been working also on the highly forbidden $6s$ to $7s$ electric dipole transition in a cesium cell but detects the ocurrence of the transition using stimulated emission rather than fluorescence [60]. The Budker group in Berkeley has been pursuing measurements in ytterbium, which has many stable isotopes available [61,62]. There is an on-going experiment in the Fortson group in Seattle using a single barium (or alternatively radium) ion [22,63]. The group of DeMille at Yale is planning to measure anapole moments by placing diatomic molecules in a strong magnetic field [64]. A collaboration in Russia wants to measure the anapole moment in a potassium cell [65]. The group at Legnaro and the current collaboration are working towards a PNC measurement using francium [66,67]. This list is not intended to encompass all the efforts, but represents some of the groups interested in PNC at present.

2 Considerations for a PNC experiment in francium

In order to enhance the small parity non-conservation effect in francium, it is necessary to perform a measurement based on an 'electroweak interference' between a weak-interaction amplitude $F_{\rm pnc}$ associated with a Z^0 exchange, and a parity conserving electromagnetic amplitude F associated with photon exchanges [49]. The means of looking for such an effect consist in preparing a handed experiment, one that can be performed in either a right-handed or a left-handed configuration. One measures the transition rate in the two configurations. The results of the two experiments differ by the electroweak interference term. A right-left asymmetry

$$A_{\rm RL} = 2\frac{{\rm Re}(F\ F_{\rm pnc})}{|F^2 + F_{\rm pnc}^2|} \tag{11}$$

can be defined. The electromagnetic amplitude is much larger than the weak-interaction amplitude and the experiments are designed to make the argument of the numerator real to maximize the effect, so the right-left asymmetry is simply:

$$A_{\rm RL} = 2\frac{F_{\rm pnc}}{F}. \tag{12}$$

Typical numbers for the asymmetry from the cesium experiments are a few parts per million [10]. The difficulty of the experiment consists in discriminating the tiny parity violating interference against parity-conserving signals that are many orders of magnitude larger. Systematic errors come from an imperfect reversal of the handedness of the experiment and give false parity violating signals that need to be checked with the help of the redundancy in the coordinate inversions.

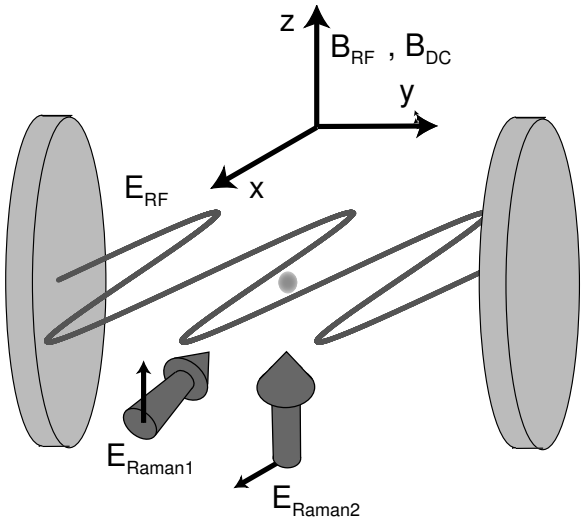

Fig. 1 Geometry of the microwave cavity setup for anapole measurements.

3 The anapole moment measurement

There is interest in measuring the anapole moment in francium. The UMD-Stony Brook-Yale group has proposed inducing microwave/RF E1 transitions between the hyperfine levels of the francium ground state [68]. Alternatively, it can be extracted from the optical measurement of $7s - 8s$ PNC-induced E1 transitions involving different hyperfine states. The transition that is forbidden by the selection rules becomes allowed due to the weak interactions that create the anapole moment. The measurement of the anapole moment gives information on the weak nucleon-nucleon interactions inside the nucleus. A measurement of the anapole moment in a chain of isotopes should provide information to separate the anapole moment due to the valence proton from that of the neutron. The constraints that could be obtained for the proton and the neutron weak anapole moments depend on the theoretical model, but in a ‘ naive picture of valence-only anapoles, they are almost orthogonal in the weak meson-nucleon coupling space [52,68].

3.1 The microwave/RF experiment

The proposal is to directly excite microwave electric dipole (E1) transitions within the ground state hyperfine manifold. The transition is parity forbidden, but is allowed by the anapole induced mixing of opposite parity states. The proposal would place $\approx 10^6$ trapped atoms at the anti-node of a standing microwave field of a Fabry-Perot resonator (for details of the geometry, see Fig. 1). The atoms must be well localized within the anti-node of the electric standing wave (microwave frequency $\nu_m \sim 45$ GHz and wavelength $\lambda_m \sim 6.6$ mm for francium). This could be accomplished by confining the atoms with a blue-detuned optical dipole trap which would minimize the perturbation of the atoms by the light field. The signal, PNC transitions, would be amplified by interfering it with a parity allowed Raman transition in the presence of a static magnetic field. Raman transitions are a convenient optical way to prepare a coherent superposition of the two levels in the hyperfine manifold, by an off-resonance 2-photon stimulated absorption-emission laser pulse using an intermediate excited state.

The fields present would define the system of coordinates for the experiment. The observable would be given by $i(\boldsymbol{E}_M \times (\boldsymbol{E_1} \times \boldsymbol{E_2})) \cdot \boldsymbol{B}$, with $\boldsymbol{E}_M$ the microwave electric field, $\boldsymbol{E}_1$ and $\boldsymbol{E}_2$ the Raman fields, $\boldsymbol{B}$ the static magnetic field and the i is present in accordance with time reversal symmetry.

3.1.1 Estimate of the anapole induced E1 transition

The anapole moment induces a small mixing of electronic states of opposite parity. The effect of the anapole moment Hamiltonian on the ground state hyperfine levels is

$$|s\bar{F}m\rangle = |sFm\rangle + \sum_{F'm'} \frac{\langle pF'm'|\boldsymbol{H_a}|sFm\rangle}{E_p - E_s}|pF'm'\rangle, \tag{13}$$

where E_p, E_s are the energies of the p and s states respectively and

$$\boldsymbol{H_a} = |e|\boldsymbol{\alpha} \cdot \boldsymbol{a}\, \delta(\boldsymbol{r}), \tag{14}$$

is the anapole moment Hamiltonian from Eq. 5 and $\boldsymbol{a}$ the anapole moment from Eq. 9.

The anapole moment mixes only states with the same F and m. For ^{209}Fr ground state, we obtain

$$|s\bar{F}m\rangle = |sFm\rangle - i\,5.9 \times 10^{-13}\,\kappa_a(F(F+1) - 25.5)\,|pFm\rangle. \tag{15}$$

The mixing coefficient is imaginary due to time reversal symmetry. In practice, the mixing is measured through the transition amplitude it induces. The presence of external electric and magnetic fields further modifies the mixing and must also be included. In the measurement considered in this propsal, the transition amplitude for ^{209}Fr between the hyperfine level F=4, m=0 and F=5, m=-1 with a microwave electric field of 100 V/cm oscillating along the x-axis (Fig. 1) and a static magnetic field of 1553 Gauss along the z-axis is

$$A_{E1}/h = \langle \bar{f}| - e\boldsymbol{E} \cdot \boldsymbol{r}|\bar{i}\rangle/h = 3.3 \times 10^{-4} i \left[\frac{E}{100\text{V/cm}}\right] \left[\frac{\kappa_a}{0.45}\right] \quad \text{Hz}. \tag{16}$$

A more accurate result can be obtained with the use of many-body methods [5,69,70]

3.1.2 Method for an anapole moment measurement

Francium atoms are initially trapped in a high-efficiency magneto-optical trap (MOT) [71], and then transferred to a second MOT in a separate chamber by means of a push beam. We then load the atoms into a dipole trap located at the electric field anti-node of a standing wave in a microwave cavity. Given all the constraints for preparation and transfer of the francium atoms, we will use a Fabry-Perot configuration for the microwave cavity (see Fig. 1).

Once the atoms are in the dipole trap we pump them into a single Zeeman sublevel. We prepare a coherent superposition of the hyperfine ground states with a Raman pulse of duration t_R. We drive the E1 transition with the cavity microwave field for a fixed time t_{E1}, and then measure the

population in the upper hyperfine level (normalized by the total number of atoms (N)) through a cycling transition. At the end of each sequence the excited state population Ξ is given by

$$\Xi_{\pm} = N|c_e|^2 = N\sin^2\left(\frac{\Omega_R t_R}{2} \pm \frac{\Omega_{E1} t_{E1}}{2}\right), \tag{17}$$

where c_e is the upper hyperfine amplitude, Ω_R and Ω_{E1} are the respective Rabi frequencies of the Raman and E1 transition, and the sign depends on the handedness of the coordinate system defined by the external fields as explained below. For a $\pi/2$ Raman pulse (or a 50-50 coherent superposition) and small Ω_{E1} this equation becomes

$$\Xi_{\pm} = N|c_e|^2 \sim N\left(\frac{1}{2} \pm \frac{\Omega_{E1} t_{E1}}{2}\right). \tag{18}$$

The second term contains the PNC signal (E1 transition) that becomes linear through the interference with the Raman transition. We measure the population transfer for both signs and define the signal as

$$\mathcal{S} = \Xi_+ - \Xi_- = N\Omega_{E1} t_{E1}. \tag{19}$$

Having the Rabi frequency for the E1 transition we can work our way back and obtain the interaction constant κ_{nsd}.

3.1.3 The apparatus and its parameters

Figure 1 shows a simplified diagram of the proposed apparatus in the ideal-case situation. The atoms (located at the origin) are prepared in a particular Zeeman sublevel $|F, m\rangle$. We apply an static magnetic field $\boldsymbol{B} = B\hat{\boldsymbol{z}}$. The atoms are excited by an standing-wave microwave electric field $\boldsymbol{E}(t) = E\cos(\nu_m t + \psi)\cos(k_m y)\hat{\boldsymbol{x}}$. The microwave frequency ν_m is tuned to the Zeeman-shifted hyperfine transition frequency ν_0. The microwave magnetic field $\boldsymbol{M}$ is deliberately aligned along $\boldsymbol{B}$; since (for a perfect standing wave) $\boldsymbol{M}$ is out of phase with $\boldsymbol{E}$, we thus have $\boldsymbol{M}(t) = M\sin(\nu_m t + \psi)\sin(k_m y)\hat{\boldsymbol{z}}$, with $M = E$ in cgs units. As we discuss below, proper alignment of $\boldsymbol{M}$ and positioning of the standing-wave node is critical for suppressing systematic effects and line-broadening mechanisms. The Raman transition is driven by two plane-wave optical fields, $\boldsymbol{E}_{R1}(t) = E_{R1}\cos(\omega_R t + \phi_R)\hat{\boldsymbol{x}}$ and $\boldsymbol{E}_{R2}(t) = E_{R2}\cos((\omega_R + \nu_m)t + \phi_R)\hat{\boldsymbol{z}}$. We assume that the Raman carrier frequency ω_R is detuned sufficiently far from optical resonance that only the vector part of the Raman transition amplitude ($\boldsymbol{V} \propto i\boldsymbol{E}_{R1} \times \boldsymbol{E}_{R2}$) is non-negligible [72]; that is, we ignore the tensor part of the Raman amplitude. In the rotating wave approximation the Raman amplitude is given by

$$A_R = \frac{E_{R1}E_{R2}}{4}\sum_{k'}\left(\frac{\langle f| - e\hat{\boldsymbol{x}}\cdot\boldsymbol{r}|k'\rangle\langle k'| - e\hat{\boldsymbol{z}}\cdot\boldsymbol{r}|i\rangle}{E_{k'} - E_s - \hbar\omega_R}\right) \tag{20}$$

The various electric and magnetic fields of the apparatus define a coordinate system related to the measured population transfer $\Xi_{\pm}$, which depends on three vectors: The polarization of the E1 transition, the polarization of the Raman transition ($\boldsymbol{V}$), and the static magnetic field $\boldsymbol{B}$ which defines magnetization of the atoms. We combine these three vectors to produce the pseudoscalar $i(\boldsymbol{E} \times (\boldsymbol{E}_{R1} \times \boldsymbol{E}_{R2}) \cdot \boldsymbol{B}$ proportional to the measured quantity.

The time varying fields must be all phase locked with respect to each other. The above pseudoscalar indicates the methods for changing the handedness of the measurement, a single reversal

of any of the fields will change the sign of the interference term of $\Xi_{\pm}$. Since the matrix element for the E1 transition is imaginary as required by time reversal symmetry, it will change sign under this reversal.

3.1.4 Signal-to-noise ratio

The measurement of the upper hyperfine state population collapses the state of each atom into one of the two hyperfine levels. The collapse distributes the atoms binomially between the two hyperfine levels and leads to an uncertainty in the measured excited state fraction called projection noise [73,74]. The projection noise is $\mathcal{N}_P = \sqrt{N|c_e|^2(1-|c_e|^2)}$, where $|c_e|^2$ is the population of the upper state. Note that the projection noise is zero when all the atoms are in one of the hyperfine levels. For a projection noise limited measurement, the signal-to-noise ratio is

$$\frac{\mathcal{S}}{\mathcal{N}_P} = 2\Omega_{E1} t_{E1} \sqrt{N}, \tag{21}$$

where t_{E1} is the duration of the E1 excitation. We want as many atoms as possible to increase the signal-to-noise ratio. With 10^6 francium atoms, which combined with Ω_{E1} given by Eq. 16, and $t_{E1} = 1$ s, gives us a signal-to-noise ratio of 4. Ω_{E1} depends linearly on κ_a, the constant we are trying to measure.

The Raman pulse can prepare initial states other than a 50-50 coherent superposition to reduce the projection noise at the expense of reducing also the signal. There are other sources of noise such as the photon shot noise, that goes as $\sqrt{N|c_e|^2}$, or technical noise that is independent of c_e. About a 50-50 initial superposition of states maximizes the signal-to-noise ratio when we include shot noise and some technical noise beyond projection noise.

While measurements in francium benefit from a large Ω_{E1}, large atomic samples of other alkalis are easily prepared. For example, while the anapole-induced parity mixing is a factor of 10 smaller in cesium than in francium, a competitive measurement with the same signal-to-noise requires a sample population 100 times larger or $N = 10^8$ for the same strength driving field. While the fundamental signal-to-noise indicates the inherent trade-offs between different alkali species, technical noise must also be considered. Systematic effects such as stray electric fields add noise to Ω_R and Ω_{E1}, and consequently a large Ω_{E1} minimizes the relative effect of technical noise sources.

3.1.5 Requirements on the apparatus

Magnetic field The stability of the static magnetic field, B_{DC}, influences the precision of the measurement. We want to drive E1 transitions between two particular Zeeman sublevels, $|F = 4, m_1\rangle \rightarrow |F = 5, m_2\rangle$. The Rabi frequencies, Ω_R and Ω_{E1}, depend on the detuning of the driving field from the energy difference of these two states. While the frequencies of the exciting fields can be well controlled, the energy difference of the Zeeman states is determined primarily by the static magnetic field.

The design of the experiment must minimize the sensitivity to magnetic field fluctuations. We can choose the static magnetic field such that the energy separation between levels goes through a minimum. At the minimum, the energy separation depends quadratically on the magnetic field.

We use the Zeeman sublevels which give the smallest quadratic dependence. The mixing of levels due to the magnetic field needs to be taken into account to calculate the E1 amplitude. The experiment can be made not only between the $|F=4,m_1\rangle, |F=5,m_2\rangle$ levels, but also between the $|F=4,m_2\rangle, |F=5,m_1\rangle$ levels, that is, interchanging m_1 and m_2, with small changes such as the state preparation where on the last step we would need to move into the other hyperfine level, the operating point of the static magnetic field and the frequency of the microwave cavity should change to account for the nuclear spin contribution to keep the measurement at the magnetic field minimum.

The frequency for the F=4, m=0 to the F=5, m=-1 transition in ^{209}Fr, expanded around the critical field $B_0 = 1553$ Gauss, is

$$\nu_m = 42.816 \times 10^9 + 90(B - B_0)^2 \text{ Hz}, \tag{22}$$

where B is in Gauss. Under this scheme, control of the magnetic field to 0.06 Gauss (three parts in 10^5) reduces the frequency noise due to magnetic field fluctuations down to $\Delta\nu_m \sim 0.3$ Hz. Similar settings will work for other Fr isotopes [68].

M1 transition The dominant transition between the two hyperfine states is a magnetic dipole (M1) transition. An M1 transition combined with other imperfections such as a misalignment of the polarization of the microwave field will mimic the parity violating signal. In our proposal, the magnetic component of the microwave field drives these transitions. In this section, we examine ways to reduce M1 transitions between the two hyperfine states.

A microwave magnetic field polarized along the x axis (see Fig. 1) has the same signature as a parity violating signal. The M1 transition amplitude between the levels of interest is given by

$$\langle \bar{f}|(-e/2m_e)(J+S)\cdot M|\bar{i}\rangle/h = 2.6 \times 10^5 \text{ Hz}, \tag{23}$$

for the maximum expected microwave magnetic field in the Fabry-Perot cavity. The ratio of the E1 transition to the M1 transition is $|A_{\rm E1}/A_{\rm M1}| \sim 1 \times 10^{-9}$. We choose to suppress it in three ways: First, we place the atoms at the magnetic field node (electric field anti-node) of the microwave cavity. If the dimension of the trap along the cavity axis is $d_t = 10$ μm, then the magnitude of the microwave magnetic field at the edges is reduced by a factor $\sin(2\pi d_t/\lambda_m)$. At 45 GHz this gives a reduction factor of 4.8×10^{-3}.

Second, we direct the polarization of the M1 field to be along the z-axis (Fig. 1). The M1 transitions in this case will be of the type $\Delta m = 0$, but the transition will not be resonant. The static magnetic field, B_{DC}, splits the magnetic sublevels of the two hyperfine levels, and the microwave field is resonant for the $|\Delta m| = 1$ E1 transitions (the microwave electric field is polarized along the x axis). The alignment will not be perfect and so we expect a suppression factor equal to $\sin(\phi) \sim \phi \sim 10^{-5}$, the angle of the microwave magnetic field polarization with respect to the z axis.

Third, the atoms in the dipole trap oscillate around the microwave magnetic field node. The change in position effectively flips the phase of the magnetic field which the atom sees, and reverses the evolution of the transition so that the transition is dynamically suppressed. The suppression will only take place if the frequency of oscillation (ζ) of the atoms inside the trap is larger than the Rabi frequency of the M1 transition. The suppression factor is given by the ratio of

these two numbers, Ω_{M1}/ζ. The frequency of oscillation along the cavity axis for our geometry is $\zeta \sim 300$ Hz.

Taken together, the three suppression mechanism reduce the expected M1 transition amplitude to $A(M1)_s/h = 5 \times 10^{-7}$ Hz. This is about 0.15% the amplitude for the E1 transition.

Dipole trap We consider a dipole trap (see Ref. [75,76] for reviews of recent work) which confines the atomic sample to a volume with a 10 μm length along the cavity axis, and a 1 mm diameter in the radial dimension with far red or blue detuned light. Since we will use 10^6 atoms for the measurement, the density of the atomic sample is 10^{11} cm^{-3}. The density is sufficiently high that care must be taken to avoid light-assisted collisions which become significant at densities as low as 10^{10} cm^{-3} [77]. The use of a far detuned trap will minimize these effects.

The depth of the confining potential must be at least ten times the average temperature of the atoms to avoid losses through evaporation. A study of the differential AC Stark shifts of the two hyperfine transitions based on the work by Romalis *et al.* [12] shows that for a blue detuned trap operating at 1.5 times the frequency of the D_1 line the differential shift is less than 3 Hz. The photon scattering rate (from Rayleigh and Raman contributions) is less than one per second.

The combination of an intensity gradient for the dipole trap and the Stark shift will introduce too much broadening in our signal for a red detuned trap. The use of a blue trap will reduce this effect because the atoms move to the dark region [78,76].

The microwave cavity We choose to provide a standing wave microwave field with a Fabry-Perot cavity. At the Fr frequency of ≈ 45 GHz, the wavelength of the excitation field is $\lambda_m \sim 0.66$ cm. The cavity will have a mirror separation of $d \sim 20\lambda_m \sim 13$ cm. In order to minimize diffraction losses, we choose a mirror radius of r_m=3.5 cm, which gives a Fresnel number $F_N > 1$, where $F_N = r_m^2/\lambda_m d$ [79]. The expected quality factor (Q) for this Fabry-Perot is $Q = 2.1 \times 10^5$. Once the cavity is coupled (loaded), the Q is reduced, and for critical coupling the loaded Q is half of the unloaded Q. The expected loaded Q is about 5×10^4. A waist of 1 cm for the cavity is enough to cover the 1mm diameter of the atom cloud. We choose a radius of curvature of R_m=9.9 cm for the cavity mirrors to ensure stability. Due to the curvature of the wavefronts, the atoms will feel an small gradient on the polarization of the microwave field. The gradient is smaller than 3×10^{-5} rad cm^{-1} over the volume of the trap.

3.2 An optical experiment as a possible alternative anapole moment measurement

So far, there has been no parity non-conservation measurement in neutral atoms performed utilizing the new technologies of laser cooling and trapping. In order to create a road-map for an experiment one could assume a transition rate measurement following closely the technique used by the Boulder group in cesium [67]. We start with a Stark shift to induce a parity conserving amplitude between the $7s$ and $8s$ levels of francium and look how this electromagnetic term will interfere with the weak interaction amplitude giving rise to a left-right asymmetry with respect to the system of coordinates defined by the static electric field **E**, static magnetic field **B**, and the Poynting vector **S** of the excitation field, such that the observable is proportional to $\mathbf{B} \cdot (\mathbf{S} \times \mathbf{E})$.

Francium atoms would accumulate in a magneto-optic trap (MOT). Then, after further cooling to control their velocities, they would be transferred to another region where a dipole trap will keep them ready for the measurement, which would be performed by moving the dipole trap with the atoms into the mode of a high finesse interferometer tuned to the $7s$ to $8s$ transition in a region with a DC electric field present. If an atom gets excited it will decay via the $7p$ state, but could also be ionized. Optical pumping techniques allow one to recycle the atom that has performed the parity non-conserving transition many times enhancing the probability to detect the signature photon. Redundancy in the reversal of the coordinates would suppress systematic errors. There is a strong assumption implicit in this statement that needs to be thoroughly studied: the trap does not affect the measurement.

3.2.1 Signal-to-noise ratio

To estimate the requirements for a parity non-conservation measurement in francium it is good to take the Boulder Cs experiment as a guide (see article by C. Wieman in reference [80]). The most important quantity to estimate is the signal-to-noise ratio since that will determine many of the requirements of the experiment.

The approach of Stark mixing works as an amplifier in the full sense of the word, it enlarges the signal, but it also brings noise. The Stark-induced part of the signal in photons per second is given in equation 24, this signal will contribute the shot noise to the measurement,

$$S_{\text{stark}} = \frac{16\pi^3}{3h\epsilon_o\lambda^3} E^2\beta^2 I_o N. \tag{24}$$

The parity non-conservation signal in photons per second is

$$S_{\text{pnc}} = \frac{16\pi^3}{3h\epsilon_o\lambda^3} 2E\beta\ \text{Im}(E_{\text{pnc}}) I_o N, \tag{25}$$

where β is the vector Stark polarizability, E is the dc electric field used for the Stark mixing interference, N the number of atoms in the interaction volume, λ the wavelength of the transition, $\text{Im}(E_{\text{pnc}})$ is the parity non-conservation amplitude expressed as an equivalent electric field, and I_o the normalized (to atomic saturation) intensity of the excitation source. Assuming only shot noise as the dominant source of noise, the signal to noise ratio achieved in one second is:

$$\frac{S_{\text{pnc}}}{N_{\text{noise}}} = 2\left(\frac{16\pi^3}{3h\epsilon_o\lambda^3}\right)^{1/2} \text{Im}(E_{\text{pnc}})\sqrt{I_o N}. \tag{26}$$

For francium in the $7s$ to $8s$ state, the ratio becomes

$$\frac{S_{\text{pnc}}}{N_{\text{noise}}} = 7.9\times 10^3\ \text{Im}(E_{\text{pnc}})\sqrt{I_o N}. \tag{27}$$

This last expression gives a result in $(\sqrt{\text{Hz}})^{-1}$ when using atomic units for the PNC term. It illustrates where a future measurement with francium is stronger: The size of the effect. The calculated value from Dzuba *et al.* [50] for $\text{Im}(E_{\text{pnc}})$ of 1.5×10^{-10} in atomic units is eighteen times larger than in cesium.

The ratio does not depend on the particular details of the interference experiment used; that is, the value of the vectorial Stark polarizability of the $7s \rightarrow 8s$ transition β nor the particular value

of the DC electric field chosen. These factors enter in the signal-to-noise ratio once the technical noise is considered.

The very high intensities available in a standing wave will exert a repelling force that will tend to move the cold atoms to a region of low intensity. FM modulation at integers of the free spectral range of the cavity can create a slowly moving travelling envelope to solve this problem as already suggested by the Boulder group. Another possible complication is the ionization of the Fr atoms that have been excited by a second photon of 507 nm. Taking a typical ionization cross section of 10^{-17} cm^2 and an intracavity intensity of 10^6 W/cm^2 the resulting ionization rate could be comparable to the decay rate from the $8S$ to the $7P$ state. Ionization during the measurement period will reduce the available atoms, and at the same time provides an efficient means of detecting the PNC signal. A careful balance between intracavity power and signal-to-noise ratio will be needed to find the optimal operating point.

3.3 Preparations and off-line work

Experience gained with francium work at Stony Brook makes clear that on-site and off-site work with a stable atom is essential for the success of the project. We are currently pursuing such work with stable Rb. Although the PNC effect is roughly 50 times smaller than in Fr, and hence the likelihood of a competitive Rb measurement is small, it allows us to understand our apparatuses and methods.

3.4 Extraction of the weak meson-nucleon couplings

The experiment measures the difference in transition rate between hyperfine levels for right and left handed coordinate systems. The measurement gives the mixing of states produced by the weak interaction, which is proportional to the effective constant $\kappa_{\rm nsd}$. The effective constant of the anapole moment κ_a can be obtained after subtracting the other two contributions to $\kappa_{\rm nsd}$ (see Eq. 6). The anapole moment of the even-neutron isotopes comes only from the unpaired proton, while the odd-neutron isotopes contain contributions from the unpaired proton and neutron. A measurement of the anapole moment to better than 10% will give a separation of both contributions. The effective constant of the anapole moment, κ_a, is related to the weak meson-nucleon couplings, and the measurement will further constrain their values [52]. The constraints obtained with the odd and even neutron isotopes are different on the the meson-nucleon coupling space [4]. Extraction and understanding of the nuclear parameters will require an equivalent effort from theorists to improve their calculations of both the atomic and nuclear physics involved.

4 Expected time-line and shift requirements

The francium project has four major phases: (i) francium trapping and basic spectroscopy; E1010, *Hyperfine anomalies in Fr*, has been approved with high priority, with shifts not granted until yields are known, and will be a milestone of this phase. (ii) transfer of Fr sample into the PNC apparatus environment. (iii) observation of the PNC signal (microwave/RF or optical). (iv) isotopic chain measurements, careful study of systematic effects.

The microwave/RF experiment could be operated with a minimum beam flux of 10^7 Fr atoms per second, i.e. quite modest proton currents on the ISAC target. We estimate that an optical experiment would be possible with $\gtrsim 10^8$ Fr atoms delivered per second.

Phase	duration (years)	shifts (12 hrs)
(i)	2	60
(ii)	1	20
(iii)	2	100
(iv)	3	150

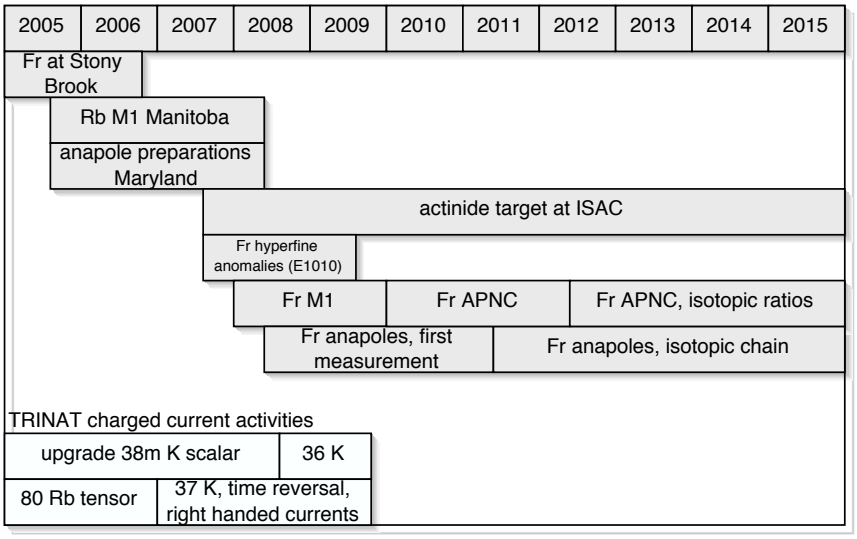

Fig. 2 A possible timetable for francium activities and the beta decay experiments at TRINAT.

References

1. Marie-Anne Bouchiat and Claude Bouchiat. Parity violation in atoms. *Rep. Prog. Phys.*, 60:1351, 1997.

2. Y. B. Zel'dovich. Parity nonconservation in the 1st order in the weak-interaction constant in electron scattering and other effects. *Sov. Phys.-JETP*, 9:682, 1959.

3. V. V. Flambaum, I. B. Khriplovich, and O. P. Sushkov. Nuclear anapole moments. *Phys. Lett. B*, 146:367, 1984.

4. W. C. Haxton and C. E. Wieman. Atomic parity nonconservation and nuclear anapole moments. *Annu. Rev. Nucl. Part. Sci.*, 51:261, 2001.

5. W. R. Johnson, M. S. Safronova, and U. I. Safronova. Combined effect of coherent Z exchange and the hyperfine interaction in the atomic parity-conconserving interaction. *Phys. Rev. A*, 67:062106, 2003.

6. J. S. M. Ginges and V. V. Flambaum. Violations of fundamental symmetries in atoms and tests of unification theories of elementary particles. *Phys. Rep.*, 397:63, 2004.

7. Y. B. Zel'dovich. Electromagnetic interaction with parity violation. *Sov. Phys.-JETP*, 6:1184, 1958.

8. P. A. Vetter, D. M. Meekhof, P. K. Majumder, S. K. Lamoreaux, and E. N. Fortson. Precise test of electroweak theory from a new measurement of parity nonconservation in atomic thallium. *Phys. Rev. Lett.*, 74:2658, 1995.

9. C. S. Wood, S. C. Bennett, D. Cho, B. P. Masterson, J. L. Roberts, C. E. Tanner, and C. E. Wieman. Measurement of parity nonconservation and an anapole moment in cesium. *Science*, 275:1759, 1997.

10. C. S. Wood, S. C. Bennett, J. L. Roberts, D. Cho, and C. E. Wieman. Precision measurement of parity nonconservation in cesium. *Can. J. Phys.*, 77:7, 1999.

11. J. M. Grossman, L. A. Orozco, M. R. Pearson, J. E. Simsarian, G. D. Sprouse, and W. Z. Zhao. Hyperfine anomaly measurements in francium isotopes and the radial distribution of neutrons. *Phys. Rev. Lett.*, 83:935, 1999.

12. M. V. Romalis and E. N. Fortson. Zeeman frequency shifts in an optical dipole trap used to search for an electric-dipole moment. *Phys. Rev. A*, 59:4547, 1999.

13. C. Chin, V. Leiber, V. Vuletic, A. J. Kerman, and S. Chu. Measurement of an electron's electric dipole moment using Cs atoms trapped in optical lattices. *Phys. Rev. A*, 63:033401, 2001.

14. S. Sanguinetti, J. Guéna, M. Lintz, P. Jacquier, A. Wasan, and M.-A. Bouchiat. Prospects for forbidden-transition spectroscopy and parity violation measurements using a beam of cold stable or radioactive atoms. *Euro. Phys. J. D*, 25:3, 2003.

15. C. E. Loving and P. G. H. Sandars. On the feasibility of an atomic-beam resonance experiment sensitive to the nuclear-spin-dependent weak neutral current interaction. *J. Phys. B*, 10:2755, 1977.

16. V. G. Gorshkov, V. F. Ezhov, M. G. Kozlov, and A. I. Mikhailov. P-odd effects in transitions between the components of the hyperfine structure of hydrogen, potassium, and cesium. *Sov. J. Nucl. Phys.*, 48:867, 1988.

17. D. Budker. *Physics Beyond the Standard Model*. World Scientific, Singapore, 1998.

18. V. E. Balakin and S. I. Kozhemyachenko. Possibility of measuring the weak interaction in the hfs transitions of atoms. *JETP Lett.*, 31:297, 1980.

19. V. N. Novikov and I. B. Khriplovich. Parity nonconservation in transitions between hyperfine structure components of heavy atoms. *JETP Lett.*, 22:74, 1975.

20. E. A. Hinds and V. W. Hughes. Parity nonconservation in hydrogen involving magnetic-electric resonance. *Phys. Lett. B*, 67:487, 1977.

21. E. G. Adelberger, T. A. Trainor, E. N. Fortson, T. E. Chupp, D. Holmgren, M Z. Iqbal, and H. E. Swanson. A technique for measureing parity non-conservation in hydrogenic atoms. *Nuc. Instr. and Meth.*, 179:181, 1981.

22. N. Fortson. Possibility of measuring parity nonconservation with a single trapped atomic ion. *Phys. Rev. Lett.*, 70:2383, 1993.

23. N. Fortson. Nuclear-structure effects in atomic parity nonconservation. *Phys. Rev. Lett.*, 765:2857, 1990.

24. W. C. Haxton. Atomic parity violation and the nuclear anapole moment. *Science*, 275:1753, 1997.

25. C. S. Wu, E. Ambler, R. W. Hayward, D. D. Hoppes, and R. P. Hudson. Experimental test of parity conservation in beta decay. *Phys. Rev.*, 105:1413, 1957.

26. R. L. Garwin, L. M. Lederman, and M. Weinrich. Observations of the failure of conservation of parity and charge conjugation in meson decays: the magnetic moment of the free muon. *Phys. Rev.*, 105:1415, 1957.

27. J. I. Friedman and V. L. Telegdi. Nuclear emulsion evidence for parity nonconservation in the decay chain $\pi^{\pm} \rightarrow \mu^{\pm} \rightarrow e^{\pm}$. *Phys. Rev.*, 106:1681, 1957.

28. S. Weinberg. *Phys. Rev. Lett.*, 19:1264, 1967.

29. N. Svartholm, editor. *Elementary Particle Theory: Relativistic Groups and Analyticity (8th Nobel Symp.)*, Amsterdam, 1968. Almqvist and Wicksell.

30. S. L. Glashow. *Nucl. Phys.*, 22:579, 1961.

31. Gargamelle Collaboration, F. J. Hasert et al. Search for elastic muon-neutrino electron scattering. *Phys. Lett. B*, 46:121, 1973.

32. L. M. Barkov and M. S. Zolotorev. Observation of nonconservation of parity in atomic transitions. *JETP Lett.*, 27:357, 1978.

33. L. M. Barkov and M. S. Zolotorev. Measurement of optical-activity of bismuth vapor. *JETP Lett.*, 28:503, 1978.

34. L. M. Barkov and M. S. Zolotorev. Parity violation in atomic bismuth. *Phys. Lett. B*, 85:308, 1979.

35. P. H. Bucksbaum, E. D. Commins, and L. R. Hunter. Observations of parity non-conservation in atomic thallium. *Phys. Rev. D*, 24:1134, 1981.

36. C. Y. Prescott, W. B. Atwood, R. L. A. Cottrell, H. DeStaebler, E. L. Garwin, A. Gonidec, R. H. Miller, L. S. Rochester, T. Sato, D. J. Sherden, C. K. Sinclair, S. Stein, R. E. Taylor, J. E. Clendenin, V. W. Hughes, N. Sasao, K. P. Schöttler, M. G. Borghini, K. Löbelsmeyer, and W. Jentschke. Parity non-conservation in inelastic electron scattering. *Phys. Lett. B*, 77:347, 1978.

37. UA1 collaboration, G. Arnison et al. Experimental observation of isolated large transverse energy electrons with associated missing energy at $\sqrt{s}$=540 GeV. *Phys. Lett. B*, 122:103, 1983.

38. UA1 collaboration, G. Arnison et al. Experimental observation of lepton pairs of invariant mass around 95 GeV/c^2 at the cern sps collider. *Phys. Lett. B*, 126:398, 1983.

39. A. Derevianko. Reconciliation of the measurement of parity nonconservation in Cs with the standard model. *Phys. Rev. Lett.*, 85:1618, 2000.

40. A. I. Milstein and O. P. Sushkov. Parity nonconservation in heavy atoms: The radiative correction enhanced by the strong electric field of the nucleus. *Phys. Rev. A*, 66:022108, 2002.

41. W. R. Johnson, I. Bednyakov, and G. Soff. Vacuum-polarization corrections to the parity-nonconserving 6s-7s transition amplitude in ^{133}Cs. *Phys. Rev. Lett.*, 87:233001, 2001.

42. M. Yu. Kuchiev and V. V. Flambaum. QED radiative corrections to parity nonconservation in heavy atoms. *Phys. Rev. Lett.*, 89:283002, 2002.

43. A. I. Milstein, O. P. Sushkov, and I. S. Terekhov. Radiative corrections and parity nonconservation in heavy atoms. *Phys. Rev. Lett.*, 89:283003, 2002.

44. P. Langacker, M. Luo, and A. K. Mann. *Rev. Mod. Phys.*, 64:87, 1992.

45. M. E. Peskin and T. Takeuchi. New constraint on a strongly interacting Higgs sector. *Phys. Rev. Lett.*, 65:964, 1990.

46. M. E. Peskin and T. Takeuchi. Estimation of oblique electroweak corrections. *Phys. Rev. D*, 46:381, 1992.

47. CDF collaboration, F. Abe et al. Search for new gauge bosons decaying into dileptons in $\bar{p}p$ collisions at $\sqrt{s}$ = 1.8 TeV. *Phys. Rev. Lett.*, 79:2192, 1997.

48. K. Cheung. Constraints on electron-quark contact interactions and implications to models of leptoquarks and extra Z bosons. *Phys. Lett. B*, 517:167, 2001.

49. I. B. Khriplovich. *Parity Non-Conservation in Atomic Phenomena*. Gordon and Breach, New York, 1991.

50. V. A. Dzuba, V. V. Flambaum, and O. P. Sushkov. Calculation of energy levels, E1 transition amplitudes, and parity violation in francium. *Phys. Rev. A*, 51:3454, 1995.

51. M. S. Safronova and W. R. Johnson. High-precision calculation of the parity-nonconserving amplitude in francium. *Phys. Rev. A*, 62:022112, 2000.

52. V. V. Flambaum and D. W. Murray. Anapole moment and nucleon weak interactions. *Phys. Rev. C*, 56:1641, 1997.

53. M. A. Bouchiat and C. Bouchiat. Parity violation induced by weak neutral currents in atomic physics 1. *J. Phys. (Paris)*, 35:899, 1974.

54. M. A. Bouchiat and C. C. Bouchiat. Weak neutral currents in atomic physics. *Phys. Lett. B*, 48:111, 1974.

55. M. A. Bouchiat and C. Bouchiat. Parity violation induced by weak neutral currents in atomic physics 2.

56. M. A. Bouchiat and C. Bouchiat. An atomic linear stark shift violating P but not T arising from the electroweak nuclear anapole moment. *Eur. Phys. J. D*, 15:5, 2001.

57. M. J. D. Macpherson, K. P. Zetie, R. B. Warrington, D. N. Stacey, and J. P. Hoare. Precise measurement of parity nonconserving optical rotation at 876 nm in atomic bismuth. *Phys. Rev. Lett.*, 67:2784.

58. D. M. Meekhof, P. Vetter, P. K. Majumder, S. K. Lamoreaux, and E. N. Fortson. High-precision measurement of parity nonconserving optical rotation in atomic lead. *Phys. Rev. Lett.*, 71:3442, 1993.

59. D. M. Meekhof, P. Vetter, P. K. Majumder, S. K. Lamoreaux, and E. N. Fortson. Optical-rotation technique used for a high-precision measurement of parity nonconservation in atomic lead. *Phys. Rev. A*, 52:1895, 1995.

60. J. Guéna, D. Chauvat, Ph. Jacquier, E. Jahier, M. Lintz, S. Sanguinetti, A. Wasan, M. A. Bouchiat, A. V. Papoyan, and D. Sarkisyan. New manifestation of atomic parity violation in cesium: A chiral optical gain induced by linearly polarized $6s - 7s$ excitation. *Phys. Rev. Lett.*, 90:143001, 2003.

61. D. DeMille. Parity nonconservation in the $6s^2\,{}^1s_0 \rightarrow 6s5d^3d_1$ transition in atomic ytterbium. *Phys. Rev. Lett.*, 74:4165, 1995.

62. J. E. Stalnaker, D. Budker, D. P. DeMille, S. J. Freedman, and V. V. Yashchuk. Measurement of the forbidden $6s2^1s_0 \rightarrow 5d6s^3d_1$ magnetic-dipole transition amplitude in atomic ytterbium. *Phys. Rev. A*, 66:031403, 2002.

63. T. W. Koerber, M. Schacht, W. Nagourney, and E. N. Fortson. Radio frequency spectroscopy with a trapped Ba^+ ion: recent progress and prospects for measuring parity violation. *J. Phys. B*, 36:637, 2003.

64. DeMille group, retrieved April 14, 2005, from http://pantheon.yale.edu/%7Edpd5/demilleresearch.htm.

65. V. F. Ezhov and M. G. Groshev and T. A. Isaev and V. V. Knjazkov and M. G. Kozlov and G. B. Krygin and N. S. Mosyagin and A. N. Petrov and S. G. Porsev and V. L. Ryabov and A. V. Titov, retrieved April 22, 2005, from http://www.qchem.pnpi.spb.ru/publication/Report01/rep.html.

66. S. N. Atutov, R. Calabrese, V. Guidi, B. Mai, E. Scansani, G. Stancari, L. Tomassetti, L. Corradi, A. Dainelli, V. Biancalana, A. Burchianti, C. Marinelli, E. Mariotti, L. Moi, and S. Veronesi. Cooling and trapping of radioactive atoms: the Legnaro francium magneto-optical trap. *J. Opt. Soc. Am. B*, 20:953, 2003.

67. S. N. Atutov, R. Calabrese, and L. Moi, editors. *Trapped Particles and Fundamental Physics, Les Houches 2000*, Amsterdam, 2002. Kluwer Academic Publishers.

68. E. Gomez, S. Aubin, L. A. Orozco, G. D. Sprouse, and D. DeMille. Measurement method for the nuclear anapole moment of laser trapped alkali atoms. *arXiv:physics/0412124*, 2004.

69. S. G. Porsev and M. G. Kozlov. Calculation of the nuclear spin-dependent parity-nonconserving amplitude for the $(7s, f = 4) \rightarrow (7s, f = 5)$ transition in Fr. *Phys. Rev. A*, 64:064101, 2001.

70. C. Bouchiat and C. A. Piketty. Nuclear-spin dependent parity violating electron nucleus interaction in heavy-atoms - the anapole moment and the perturbation of the hadronic vector neutral current by the hyperfine interaction. *Phys. Lett. B*, 269:195, 1991.

71. S. Aubin, E. Gomez, L. A. Orozco, and G. D. Sprouse. High efficiency magneto-optical trap for unstable isotopes. *Rev. Sci. Instrum.*, 74:4342, 2003.

72. D. DeMille and M. G. Kozlov. Stark-induced electric dipole amplitudes for hyperfine transitions. *arXiv:*, physics:9801034, 1998.

73. W. M. Itano, J. C. Begquist, J. J. Bollinger, J. M. Gilligan, D. J. Heinzen, F. L. Moore, M. G. Raizen, and D. J. Wineland. Quantum projection noise: Population fluctuations in two-level systems. *Phys. Rev. A*, 47:3554, 1993.

74. W. M. Itano, J. C. Begquist, J. J. Bollinger, J. M. Gilligan, D. J. Heinzen, F. L. Moore, M. G. Raizen, and D. J. Wineland. Erratum: Quantum projection noise: Population fluctuations in two-level systems. *Phys. Rev. A*, 51:1717, 1995.

75. V. I. Balykin, V. G. Minogin, and V. S. Letokhov. Electromagnetic trapping of cold atoms. *Rep. Prog. Phys.*, 63:1429, 2000.

76. N. Friedman, A. Kaplan, and N. Davidson. *Advances in Atomic, Molecular, and Optical Physics*, 48:99, 2002.

77. K. Suominen, K. Burnett, P. S. Julienne, M. Walhout, U. Sterr, C. Orzel, M. Hoogerland, and S. L. Rolston. Ultracold collisions and optical shielding in metastable xenon. *Phys. Rev. A*, 533:1678, 1996.

78. S. Kulin, S. Aubin, S. Christe, B. Peker, S. L. Rolston, and L. A. Orozco. A single hollow-beam optical trap for cold atoms. *J. Opt. B: Quantum Semiclass. Opt.*, 3:353, 2001.

79. S. Ramo, J. F. Whinnery, and T. Van Duzer. *Fields and Waves in Communication Electronics*. John Wiley and Sons, New York, 1993.

80. P. Langacker, editor. *Precision Tests of the Standard Electroweak Model*. World Scientific, Singapore, 1995.

Include publications in refereed journal over at least the previous 5 years.

1. Enhancement of low energy electron ion recombination in a magnetic field: Influence of transient field effects.
   M. Hörndl , S. Yoshida, A. Wolf, G. Gwinner, J. Burgdörfer.
   Accepted for publication in Physical Review Letters.

2. Experimental tests of time dilation in special relativity.
   G. Gwinner.
   Modern Physics Letters A 20, 791 (2005).

3. TITAN project status report and a proposal for a new cooling method of highly charged ions.
   V.L. Ryjkov, L. Blomeley, M. Brodeur, P. Grothkopp, M. Smith, P. Bricault, F. Buchinger, J. Crawford, G. Gwinner, J. Lee, J. Vaz, G. Werth, J. Dilling, and the TITAN Collaboration.
   Eur. Phys. J A direct (2005): epjad/i2005-06-122-1

4. Hyperfine quenching of resonances in dielectronic recombination of zinc-like Pt^{48+}.
   S. Schippers, G. Gwinner, C. Brandau, S. Böhm, M. Grieser, S. Kieslich, H. Knopp, A. Müller, R. Repnow, D. Schwalm, and A.Wolf.
   Nucl. Instrum. Methods B 235, 265 (2005).

5. A new measurement of the decay rate of the negative positronium ion: status and preliminary results.
   F. Fleischer, K. Degreif, G. Gwinner, M. Lestinsky, V. Liechtenstein, F. Plenge, H. Scheit, D. Schwalm.
   Canadian Journal of Physics. 83, 413 (2005).

6. Test of time dilation by laser spectroscopy on fast ions.
   G. Saathoff, S. Reinhardt, H. Buhr, L.A. Carlson, D. Schwalm, A. Wolf, S. Karpuk, C. Novotny, G. Huber, G. Gwinner.
   Canadian Journal of Physics. 83, 425 (2005).

7. Dielectronic recombination resonances in Na^{8+}.
   D. Nikolic, E. Lindroth, S. Kieslich, C. Brandau, S. Schippers, W. Shi, A. Müller, G. Gwinner, M. Schnell, A. Wolf.
   Phys. Rev. A 70, 062723 (2004).

8. Determination of the 2s-2p excitation energy of lithiumlike scandium using dielectronic recombination.
   S. Kieslich, S. Schippers, W. Shi, A. Müller, G. Gwinner, M. Schnell, A. Wolf, E. Lindroth, M. Tokman.
   Physical Review A 70, 042714 (2004).

9. Towards a new measurement of the decay rate of the negative positronium ion Ps^-.
   D. Schwalm, F. Fleischer, M. Lestinsky, K. Degreif, G. Gwinner, V. Liechtenstein, F. Plenge, H. Scheit.
   Nucl. Instr. and Meth. B 221, 185 (2004).

10. Improved test of time dilation in special relativity.
    G. Saathoff, S. Karpuk, U. Eisenbarth, G. Huber, S. Krohn, R. Muñoz Horta, S. Reinhardt, D. Schwalm, A. Wolf, and G. Gwinner.
    Phys. Rev. Lett. 91, 190403 (2003).

11. Absolute high-resolution rate coefficients for dissociative recombination of electrons with HD^+: Comparison of results from three heavy-ion storage rings.
A. Al-Khalili, S. Rosen, H. Danared, A. M. Derkatch, A. Källberg, M. Larsson, A. Le Padellec, A. Neau, J. Semaniak, R. Thomas, M. af Ugglas, L. Vikor, W. Zong, W. J. van der Zande, X. Urbain, M. J. Jensen, R. C. Bilodeau, O. Heber, H. B. Pedersen, C. P. Safvan, L. H. Anderson, M. Lange, J. Levin, G. Gwinner, L. Knoll, M. Scheffel, D. Schwalm, R. Wester, D. Zajfman, and A. Wolf.
Phys. Rev. A 68, 042702 (2003).

12. Heavy-ion storage ring quest for atomic lifetimes of Li^+ and Be^{2+}.
E. Träbert, G. Gwinner, E. J. Knystautas, and A. Wolf.
Can. J. Phys. 81, 941, (2003).

13. Observation of Trielectronic Recombination in Be-like Cl Ions.
M. Schnell, G. Gwinner, N. R. Badnell, M. E. Bannister, S. Böhm, J. Colgan, S. Kieslich, S. D. Loch, D. Mitnik, A. Müller, M. S. Pindzola, S. Schippers, D. Schwalm, W. Shi, A. Wolf, and S.-G. Zhou.
Phys. Rev. Lett. 91, 043001 (2003).

14. Dielectronic Recombination of Fe XXI and Fe XXII via N = 2 → N' = 2 Core Excitations.
D. W. Savin, S. M. Kahn, G. Gwinner, M. Grieser, R. Repnow, G. Saathoff, D. Schwalm, A. Wolf, A. Müller, S. Schippers, P. A. Zavodszky, M. H. Chen, T. W. Gorczyca, O. Zatsarinny, and M. F. Gu.
Astrophys. J. Suppl. Ser., 147, 421 (2003).

15. M1/E2/M2 decay rates in Fe VII, Fe IX, Fe X, and Fe XIII measured at a heavy-ion storage ring.
E. Träbert, A.G. Calamai, G. Gwinner, E. J. Knystautas, E. H. Pinnington, and A. Wolf.
J. Phys. B 36, 1129 - 1141 (2003).

16. Toward a new test of the relativistic time dilation factor by laser spectroscopy of fast ions in a storage ring.
G. Saathoff, U. Eisenbarth, S. Hannemann, I. Hoog, G. Huber, S. Karpuk, S. Krohn, J. Lassen, D. Schwalm, M. Weidemüller, A. Wolf, and G. Gwinner.
Hyperfine Interactions 146-147, 71 (2003).

17. Recombination Measurements at Ion Storage Rings.
A. Wolf and G. Gwinner.
Hyperfine Interactions 146-147, 5 (2003).

18. Laser-Cooled Ions and Atoms in a Storage Ring.
J. Kleinert, S. Hannemann, U. Eisenbarth, B. Eike, M. Grieser, R. Grimm, G. Gwinner, S. Karpuk, G. Saathoff, U. Schramm, D. Schwalm, and M. Weidemüller.
Hyperfine Interactions 146-147, 189 (2003).

19. Trielectronic recombination in Be-like ions.
M. Schnell, M.E. Bannister, S. Böhm, G. Gwinner, S. Kieslich, A. Müller, S. Schippers, D. Schwalm, W. Shi, A. Wolf, and S.G. Zhou.
Nucl. Instrum. Methods B 205, 367 (2003).

20. Dielectronic recombination at low energies: Spectroscopy of doubly excited states in berylliumlike Na^{7+} ions.

S. Kieslich, S. Böhm, C. Brandau, A. Müller, S. Schippers, W. Shi, G. Gwinner, M. Schnell, and A. Wolf.
Nucl. Instrum. Methods B 205, 99 (2003).

21. M1 transition rates from electron beam ion trap and heavy-ion storage ring.
E. Träbert, P. Beiersdorfer, G. Gwinner, E. H. Pinnington, and A. Wolf.
Nucl. Instrum. Methods B 205, 83 (2003).

22. M1 transition rate in Cl^{12+} from electron beam ion trap and heavy-ion storage ring.
E. Träbert, P. Beiersdorfer, G. Gwinner, E. H. Pinnington, and A. Wolf.
Phys. Rev. A 66, 052507 (2002).

23. Dielectronic recombination resonances in F^{6+}.
M. Tokman, N. Eklöw, P. Glans, E. Lindroth, R. Schuch, G. Gwinner, D. Schwalm, A. Wolf, A. Hoffknecht, A. Müller, and S. Schippers.
Phys. Rev. A 66, 012703 (2002).

24. Interference effects in the photorecombination of argonlike Sc^{3+} ions: storage ring experiment and theory.
S. Schippers, S. Kieslich, A. Müller, G. Gwinner, M. Schnell, A. Wolf, A. Covington, M.E. Bannister, L.B. Zhao.
Phys. Rev. A 65, 042723 (2002).

25. Dielectronic recombination (via $N = 2 \rightarrow N' = 2$ core excitations) and radiative recombination onto Fe XX: laboratory measurements and theoretical calculations.
D.W. Savin, E. Behar, S.M. Kahn, G. Gwinner, A.A. Saghiri, M. Schmitt, M. Grieser, R. Repnow, D. Schwalm, A. Wolf, T. Bartsch, A. Müller, S. Schippers, N.R. Badnell, M.H. Chen, and T.W. Gorczyca.
Astrophys. J. Suppl. Ser. 138, 337 (2002).

26. Measurement of EUV intercombination transition rates in Be-like ions at a heavy-ion storage ring.
E. Träbert, A. Wolf, and G. Gwinner.
Phys. Lett. A 295, 44 (2002).

27. M1/E2 transition rates in Fe X through Fe XIII measured at a heavy-ion storage ring.
E. Träbert, G. Gwinner, A. Wolf, E. J. Knystautas, H.-P. Garnir, X. Tordoir.
J. Phys. B: At. Mol. Opt. Phys. 35, 671 (2002).

28. M1/E2 decay rate in Ar^{2+} measured at a heavy-ion storage ring.
E. Träbert and G. Gwinner.
Phys. Rev. A 65, 014501 (2002).

29. First determination of the ionization potential of actinium and first observation of optical transitions in fermium.
H. Backe et al.
Journal of Nuclear Science and Technology, Suppl. 3, 86 (2002).

30. Lifetime of metastable Ne^{2+} ions measured at a heavy-ion storage ring.
E. Träbert, A. Wolf, X. Tordoir, E.H. Pinnington, E.J. Knystautas, G. Gwinner, A.G. Calamai, and R.L. Brooks.
Can. J. Phys. 79, 145-151 (2001).

31. Storage Ring Measurement of the C IV Recombination Rate Coefficient.
S. Schippers, A. Müller, G. Gwinner, J. Linkemann, A.A. Saghiri, and A. Wolf.
The Astrophysical Journal, 555, 1027-1037 (2001).

32. Dielectronic Recombination in iron L-shell ions.
G. Gwinner, D.W. Savin, D. Schwalm, A. Wolf, S. Schippers, A. Müller, N.R. Badnell, and M.H. Chen.
Physica Scripta T92 (2001) 319-321.

33. Photorecombination of lithiumlike Sc^{18+} at threshhold: a challenge for atomic structure theory.
S. Kieslich, S. Böhm, A. Müller, S. Schippers, W. Shi, G. Gwinner, M. Schnell, A. Wolf, E. Lindroth, M. Tokman.
Physica Scripta T92 (2001) 376-378.

34. Field enhanced dielectronic recombination of lithiumlike Ti^{19+} and Ni^{25+} ions.
S. Schippers, T. Bartsch, S. Böhm, G. Gwinner, D. Schwalm, A. Wolf, R.A. Phaneuf, R. Schuch, and A. Müller.
Physica Scripta T92 (2001) 391-394.

35. Recombination of bare Cl^{17+} ions in an electron cooler.
A. Hoffknecht, S. Schippers, A. Müller, G. Gwinner, D. Schwalm, and A. Wolf.
Physica Scripta T92 (2001) 402-405.

36. Intercombination and forbidden transition rates in C- and N-like ions (O^{2+}, F^{3+}, and S^{9+}) measured at a heavy-ion storage ring.
E. Träbert, A.G. Calamai, J.D. Gillaspy, G. Gwinner, X. Tordoir, A. Wolf.
Phys. Rev. A 62, 022507 (2000).

37. Electric quadrupole and magnetic dipole transition probabilities within the ground configuration of F^{+}.
A.G. Calamai, G. Gwinner, X. Tordoir, E. Träbert, and A. Wolf.
Phys. Rev. A 61, 062508 (2000).

38. Dielectronic recombination of lithium-like Ni^{25+} ions: high resolution rate coefficients and influence of external crossed E and B fields.
S. Schippers, T. Bartsch, C. Brandau, A. Müller,G. Gwinner, G. Wissler, M. Beutelspacher, M. Grieser, A. Wolf, and R. A. Phaneuf.
Phys. Rev. A 62, 022708 (2000).

39. Enhanced dielectronic recombination of lithium-like Ti^{19+} ions in external E x B fields.
T. Bartsch, S. Schippers, M. Beutelspacher, S. Böhm, M. Grieser, G. Gwinner, A.A. Saghiri, G. Saathoff, R. Schuch, D. Schwalm, A. Wolf, and A. Müller.
J. Phys. B 33, L453 (2000).

40. Influence of magnetic fields on electron-ion recombination at very low energies.
G. Gwinner, A. Hoffknecht, T. Bartsch, M. Beutelspacher, N. Eklöw, P. Glans, M. Grieser, S. Krohn, E. Lindroth, A. Müller, A.A. Saghiri, S. Schippers, U. Schramm, D. Schwalm, M. Tokman, G. Wissler, and A. Wolf.
Phys. Rev. Lett. 84, 4822 (2000).

41. Rate predictions for two-photon spectroscopy of highly charged ions through laser-induced recombination.
G. Saathoff, G. Gwinner, T. Kühl, D. Schwalm, H. Winter, and A. Wolf.
Hyperfine Interactions 127, 211 (2000).

42. Spectroscopy using stimulated electron-ion recombination.
A. Wolf, G. Uhlenberg, U. Schramm, T. Schüssler, A.E. Livingston, G. Gwinner, G. Saathoff, and D. Schwalm.
Hyperfine Interactions 127, 203 (2000).

43. Recombination in electron coolers.
A. Wolf, G. Gwinner, J. Linkemann, A.A. Saghiri, M. Schmitt, D. Schwalm, M. Grieser, M. Beutelspacher, T. Bartsch, C. Brandau, A. Hoffknecht, A. Müller, S. Schippers, O. Uwira, and D. Savin.
Nucl. Instr. and Meth. A 441, 183 (2000).

44. Experimental evidence for magnetic field effects on dielectronic recombination via high rydberg states.
T. Bartsch, S. Schippers, A. Müller, C. Brandau, G. Gwinner, A. A. Saghiri, M. Beutelspacher, M. Grieser, D. Schwalm, A. Wolf, H. Danared, and G. H. Dunn.
Phys. Rev. Lett. 82, 3779 (1999).

45. Magnetic dipole transition rates in B-like and F-like titanium ions measured at a heavy-ion storage ring.
E. Träbert, G. Gwinner, A. Wolf, X. Tordoir, A.G. Calamai.
Phys. Lett. A 264, 311 (1999).

46. Precise lifetime measurements on the intercombination transitions in the B-like ions C^+ and N^{2+} using a heavy-ion storage ring.
E. Träbert, G. Gwinner, E.J. Knystautas, X. Tordoir, A. Wolf.
J. Phys. B 32, L1 (1999).

47. Threshold effects and ion-pair production in the dissociative recombination of HD^+.
M. Lange, J. Levin, G. Gwinner, U. Hechtfischer, L. Knoll, D. Schwalm, R. Wester, A. Wolf, X. Urbain, and D. Zajfman.
Phys. Rev. Lett. 83, 4979 (1999).

48. Experimental investigation of the $6s^2\,{}^1S_0 \rightarrow 5d6s^3D_{1,2}$ forbidden transitions in atomic ytterbium.
C.J. Bowers, D. Budker, D. DeMille, S.J. Freedman, G. Gwinner, and J.E.Stalnaker.
Phys. Rev. A 59, 3513 (1999).

49. Ground-state hyperfine measurement in laser-trapped radioactive ^{21}Na.
M. A. Rowe, S. J. Freedman, B. K. Fujikawa, G. Gwinner, S.-Q. Shang, and P. A. Vetter.
Phys. Rev. A 59, 1869 (1999).

50. Recombination of F^{6+} with free electrons at very low energies.
A. Hoffknecht, T. Bartsch, S. Schippers, A. Müller, N. Eklöw, P. Glans, M. Beutelspacher, M. Grieser, G. Gwinner, A.A. Saghiri, and A. Wolf.
Physica Scripta T80B, 298 (1999).

51. Field enhanced dielectronic recombination of Si^{11+} and Cl^{14+} ions.
T. Bartsch, A. Müller, W. Spies, J. Linkemann, S. Schippers, C. Brandau, H. Danared, D.R. DeWitt, H. Gao, W. Zong, R. Schuch, A. Wolf, G. Gwinner, A.A. Saghiri, M. Schmitt, M. Beutelspacher, M. Grieser, and G.H. Dunn.
Physica Scripta T80B, 305 (1999).

52. Photorecombination of Sc^{3+} and Ti^{4+} ions: Search for interference effects and recombination at low energies.
S. Schippers, T. Bartsch, C. Brandau, A. Müller, G. Gwinner, J. Linkemann, A.A. Saghiri, and A. Wolf.
Physica Scripta T80B, 314 (1999).

53. Dielectronic recombination of Li-like fluorine ions.
P. Glans, E. Lindroth, N. Eklöw, W. Zong, G. Gwinner, A.A. Saghiri, M. Pajek, H. Danared, and R. Schuch.
Nucl. Instr. and Meth. B 154, 97 (1999).

54. Photorecombination of Ti^{4+} ions: search for interference effects, recombination at low energies and rate coefficient in plasmas.
S. Schippers, T. Bartsch, C. Brandau, G. Gwinner, J. Linkemann, A. Müller, A.A. Saghiri, A. Wolf.
J. Phys. B 31, 4873 (1998).

55. Magneto-optic trapping of ^{210}Fr.
J.E. Simsarian, A. Ghosh, G. Gwinner, L.A. Orozco, G.D. Sprouse, and P.A. Voytas.
Phys. Rev. Lett. 76, 3522 (1996).

56. Magnetic dipole and electric quadrupole moments of the neutron deficient bismuth isotopes.
P. Campbell, J.A. Behr, J. Billowes, G. Gwinner, G.D. Sprouse, F. Xu.
Nucl. Phys. A 598, 61 (1996).

57. Laser traps for radioactive isotopes.
P.A. Voytas, J.A. Behr, A. Ghosh, G. Gwinner, L.A. Orozco, J.E. Simsarian, G.D. Sprouse, F. Xu.
Hyperfine Interactions 97/98 529 (1996).

58. Isotope shifts of the neutron-deficient bismuth isotopes: charge radii systematics across the Z=82 shell closure.
P. Campbell, J. Billowes, J.A. Behr, G. Gwinner, G.D. Sprouse, F. Xu.
Phys. Lett. B 346, 21 (1995).

59. A low-energy ion beam from alkali heavy-ion reaction products.
J.A. Behr, S.B. Cahn, S.B. Dutta, A. Ghosh, G. Gwinner, C.H. Holbrow, L.A. Orozco, G.D. Sprouse, J. Urayama, F. Xu.
Nucl. Instr. and Meth. A 351, 256 (1994).

60. Magneto-optic trapping of radioactive ^{79}Rb.
G. Gwinner, J.A. Behr, S.B. Cahn, A. Ghosh, L.A. Orozco, G.D. Sprouse, F. Xu.
Phys. Rev. Lett. 72, 3795 (1994).

61. Possibilities for francium spectroscopy in a light trap.
J.A. Behr, S.B. Cahn, S.B. Dutta, A. Görlitz, A. Ghosh, G. Gwinner, L.A. Orozco, G.D. Sprouse, F. Xu.
Hyperfine Interactions 81, 197 (1993).

62. Optical isotope shifts of stable hafnium atoms in a resonance cell on-line with a heavy-ion accelerator.
J. Schecker, A. Berger, J. Das, S. Dutta, G. Gwinner, C.H. Holbrow, T. K§hl, T. Lauritsen, G.D. Sprouse, F. Xu.
Phys. Rev. A 46, 3730 (1992).

63. A resonance cell for on-line optical spectroscopy of accelerator produced radioactive atoms.

A. Berger, J. Billowes, J. Das, S. Dutta, G. Gwinner, C.H. Holbrow, T. K§hl, T. Lauritsen, S.L. Rolston, J. Schecker, G.D. Sprouse, F. Xu.
Nucl. Instr. and Meth. A 311, 224 (1992).

64. Laser spectroscopy of nuclear reaction products: recent results and future prospects.
J.A. Behr, S.B. Cahn, J. Das, G. Gwinner, C.H. Holbrow, T. Lauritsen, L.A. Orozco, S.Q. Shang, J. Schecker, G.D. Sprouse, F. Xu.
Hyperfine Interactions 74, 23 (1992).